International Geology Review, Vol. 39, 1997, p. 449–460.

A Brasiliano Age (500 ± 5 Ma) for the Mina III Gold Deposit, Crixás Greenstone Belt, Central Brazil[1]

PAULO DE TARSO FERRO DE OLIVEIRA FORTES,

Departamento de Geologia Geral e Aplicada (GEO), Instituto de Geociências (IG), Universidade de Brasília (UnB), Campus Universitário, Brasília, DF 70910-900, Brazil

ALAIN CHEILLETZ,

Centre de Recherches Pétrographiques e Géochimiques (CRPG-CNRS), UPRA 9046, and Ecole Nationale Supérieure de Géologie (ENSG-INPL), 15 Rue N.D. des Pauvres, B.P. 20, 54501, Vandoeuvre Cedex, France

GASTON GIULIANI,

Institut Français de Recherche Scientifique pour le Développement en Coopération (ORSTOM), and CRPG-CNRS, 213 Rue Lafayette, 75480, Paris Cedex 10, France

AND GILBERT FÉRAUD

UMR Géosciences Azur, UNR 6526, CNRS, Parc Valrose, 06108, Nice Cedex 2, France

Abstract

K-Ar and $^{40}Ar/^{39}Ar$ geochronological studies were performed on selected minerals from the Mina III gold deposit, Crixás greenstone belt, state of Goiás, central Brazil. They include amphibole and biotite from amphibole schists; biotite from quartz-chlorite-carbonate-muscovite schists; chloritoid, muscovite, and paragonite from muscovite schists; and biotite from biotite-marbles. Analyses yielded ages between 750 and 500 Ma, indicating that the Brasiliano orogenic event affected rocks of the Archean greenstone belt. It is proposed that the gold mineralization, closely related to a post-metamorphic peak hydrothermal alteration and spatially associated with muscovite schists, is 505 ± 10 Ma, whereas older ages may indicate an excess of argon.

Introduction

THE MINA III gold deposit is exploited in the underground mine of Mineração Serra Grande Ltda., which is a joint venture of Mineração Morro Velho S.A. and Inco. It is a gold-only deposit and is the largest gold mine in the state of Goiás, central Brazil, with reserves estimated at 5.2 million metric tons with an average grade of 12.8 g/t (Yamaoka and Araújo, 1988). This paper reports on a K-Ar and $^{40}Ar/^{39}Ar$ geochronological study of wall rocks of the deposit, including gangue minerals associated with the gold mineralization.

Geological Setting

The Mina III gold deposit is located in the Archean Crixás greenstone belt (Saboia, 1979) (Fig. 1) (Arndt et al., 1989), which is represented by the Córrego Alagadinho (metakomatiites), Rio Vermelho (metabasalts), and Ribeirão das Antas (chemical and pelitic metasediments) formations (Saboia et al., 1981) of the Crixás Group (Jost and Oliveira, 1991). The volcano-sedimentary sequence is bordered by Archean granite-gneissic rocks (Anta and Caiamar complexes) and is covered on the north by Proterozoic metasedimentary rocks (Araxá Group) (Fig. 2).

The Mina III gold deposit consists of a strongly deformed, metamorphosed, and hydrothermally altered sequence of rocks, consisting mainly of amphibole schists and quartz-chlorite-carbonate-muscovite schists, Fe-dolomitic marbles, carbonaceous schists, quartz-chlorite-muscovite-garnet schists, and feldspathic schists (Fig. 3). Intense hydrothermal alterations (carbonatization, sericitization, sulfidization, and silicification) are associated with two main mineralized zones that are worked out—the Upper and Lower ore zones (Yamaoka and

[1]This paper is one of a series of contributions (Marcos Zentilli, compiler) to Project No. 342, Age and Isotopes of South American Ores, of the International Geological Correlation Program.

0020-6814/97/266/449-12 $10.00

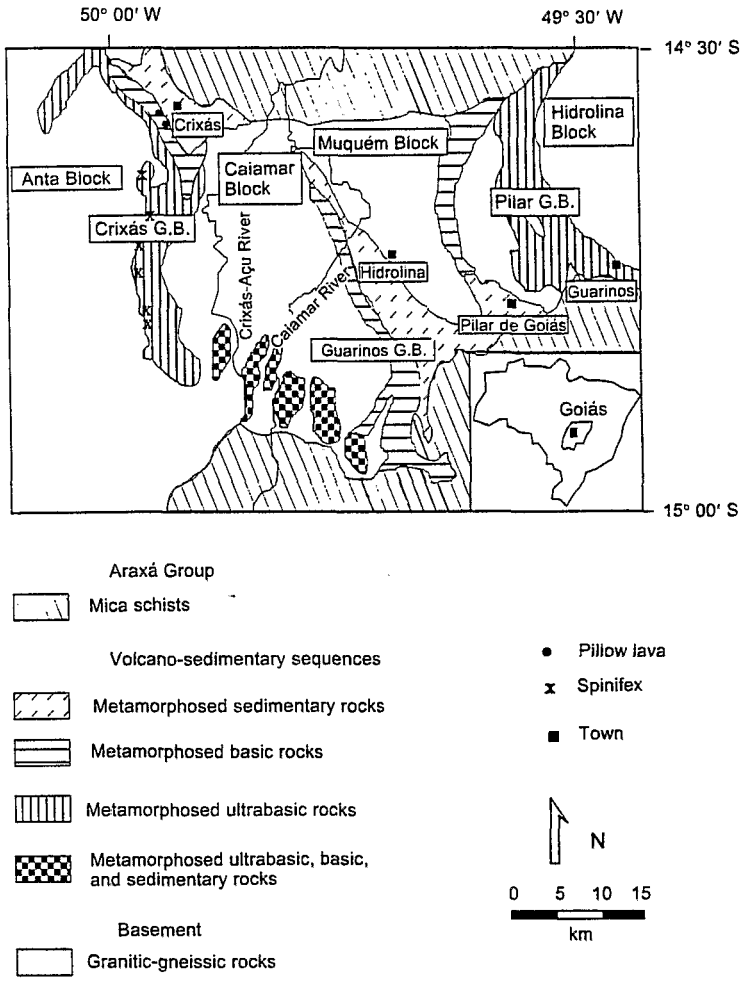

FIG. 1. Geological sketch map of the Crixás greenstone belt (from Saboia, 1979).

Araújo, 1988). They are thought to post-date the metamorphic peak of epidote-amphibolite facies (Thomson, 1986; Thomson and Fyfe, 1990).

The Upper Ore Zone consists of irregular massive sulfide bodies, 0.5 to 2.5 m in width, composed mainly of arsenopyrite and/or pyrrhotite, with minor chalcopyrite. The massive sulfides are associated with muscovite schists, chlorite-garnet schists, magnetite schists, and biotite marbles within a sequence of Fe-dolomitic marbles and quartz-chlorite-carbonate-muscovite schists (Fig. 4). Gold is preferentially included or infilled within microfractures in arsenopyrite, but is rarely included in silicates and oxides.

The Lower Ore Zone is represented either by a concordant quartz vein (0.5 to 3.0 m width) within carbonaceous schists or by an arsenopyrite- and/or pyrrhotite-bearing carbonaceous schist close to the contact with the vein (Fig. 4). Gold in the quartz vein occurs as intergranular inclusions, filling microfractures or associated with carbonaceous material disseminated in the vein. In the arsenopyrite- and/or pyrrhotite-bearing carbonaceous schist, gold is preferentially associated with arsenopyrite or included in quartz (Fortes, 1996).

Both ore zones show a strong structural control, related to intersection and/or elongation lineations parallel or subparallel to the axis of semi-recumbent and asymmetric folds. These

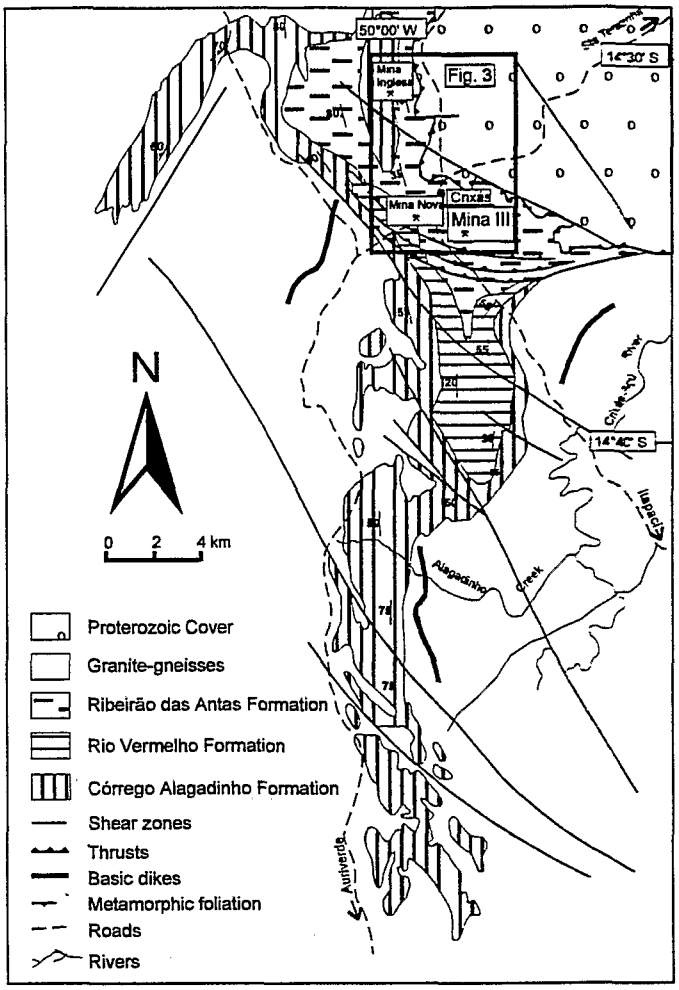

FIG. 2. Geological map of the Crixás greenstone belt (modified from Jost and Oliveira, 1991).

secondary structures were generated by ductile progressive simple shearing that also developed a penetrative axial-plane foliation (Fortes, 1996).

The amphibole schists and the quartz-chlorite-carbonate-muscovite schists are interpreted as metabasic rocks that show an increasing degree of hydrothermal alteration, mainly chloritization, carbonatization, and sericitization (K-alteration) toward mineralization. Muscovite schists and biotite-marbles are closely associated with the massive sulfide orebodies. The muscovite schists may correspond to ferriferous/aluminous metasediments or even to strongly sericitized metabasic rocks. Biotite-marbles may be related to an extreme carbonatization of metabasic rocks or to the K-alteration of pre-existing marbles (Fortes, 1996). The favored hypothesis concerning the formation of the deposit is a hydrothermal-mesothermal model associated with the development of a regional shear zone (Fortes and Giuliani, 1995; Fortes, 1996).

Petrography

The amphibole schists consist of chlorite (30 to 40%), carbonate (20 to 30%), quartz (15 to 30%), hornblende (10 to 30%), and minor biotite, epidote, plagioclase, ilmenite, and

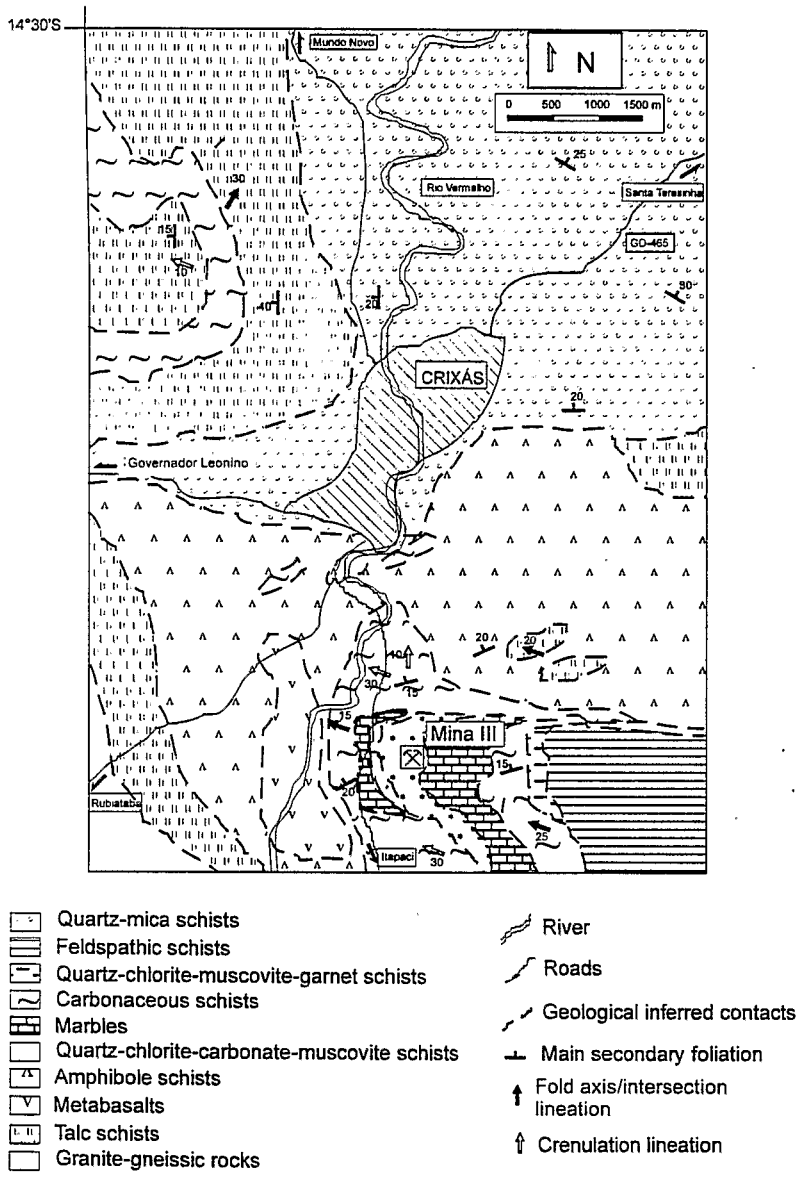

FIG. 3. Geological map of the Mina III gold deposit area (from Fortes, 1996).

pyrite. Hornblende occurs as concordant or discordant porphyroblasts (Fig. 5), whereas biotite may occur intergrown with chlorite or as discordant porphyroblasts (Fig. 6).

The quartz-chlorite-carbonate-muscovite schists consist of quartz (20 to 40%), chlorite (10 to 25%), carbonate (5 to 30%), muscovite (10 to 40%), and biotite (5 to 15%), with minor plagioclase, tourmaline, ilmenite, pyrrhotite, pyrite, and arsenopyrite. Biotite occurs as intergrowths with chlorite or as porphyroblasts concordant or discordant with the foliation (Fig. 7).

The muscovite schists consist of white mica (75 to 95%), predominantly muscovite and rarely paragonite, and minor chloritoid, garnet, plagioclase, quartz, ilmenite, hematite, arsenopyrite, pyrrhotite, pyrite, and chalcopyrite. The

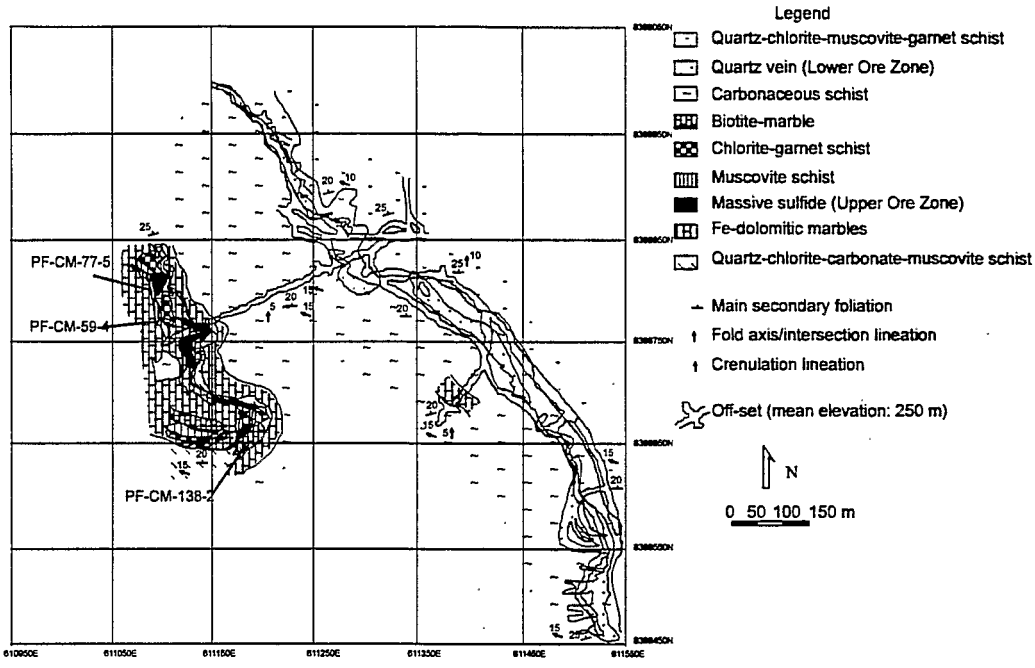

FIG. 4. Geological map of the 150-m level of the Mina III gold deposit (from Fortes, 1996).

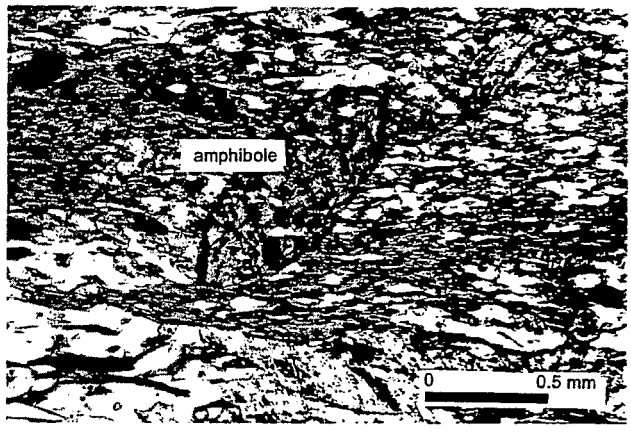

FIG. 5. Thin-section photomicrograph showing a discordant hornblende porphyroblast in amphibole schist of the Mina III gold deposit (K-60/380.20, parallel nicols).

chloritoid occurs as porphyroblasts parallel or discordant with the schistosity (Fig. 8).

The biotite-marbles consist of carbonate (70 to 90%), biotite (5 to 10%), quartz (5 to 10%), white mica (5 to 10%), and minor plagioclase, chlorite, and arsenopyrite. Biotite porphyroblasts outline the schistosity or are discordant with it (Fig. 9).

Analytical K-Ar and $^{40}Ar/^{39}Ar$ Procedure

Drill-core (K-60/380.20, K-58/351.40, K-58/275.55, and K-20/272.35) and underground mine (PF-CM-59-4, PF-CM-77-5, and PF-CM-138-2) samples representative of the different petrographic types described above were collected for this study. A total of 9 concentrates (2 amphibole, 4 biotite, 1 chloritoid,

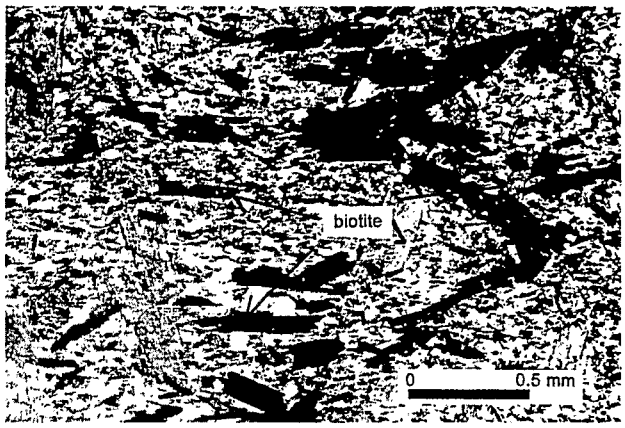

FIG. 6. Thin-section photomicrograph showing discordant biotite porphyroblasts in amphibole schist of the Mina III gold deposit (K-60/380.20, parallel nicols).

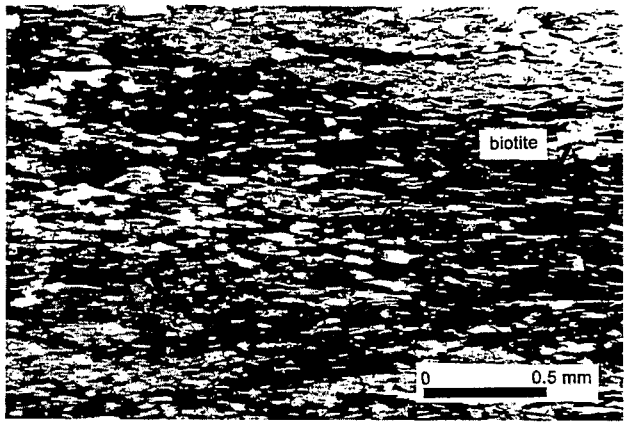

FIG. 7. Thin-section photomicrograph showing concordant and discordant biotite porphyroblasts in quartz-chlorite-carbonate-muscovite schist of the Mina III gold deposit (K-20/272.35, parallel nicols).

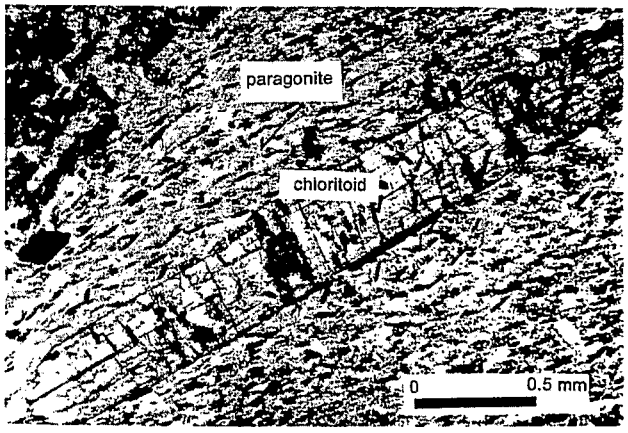

FIG. 8. Thin-section photomicrograph showing a discordant chloritoid porphyroblast in muscovite schist of the Mina III gold deposit (PF-CM-77-5, parallel nicols).

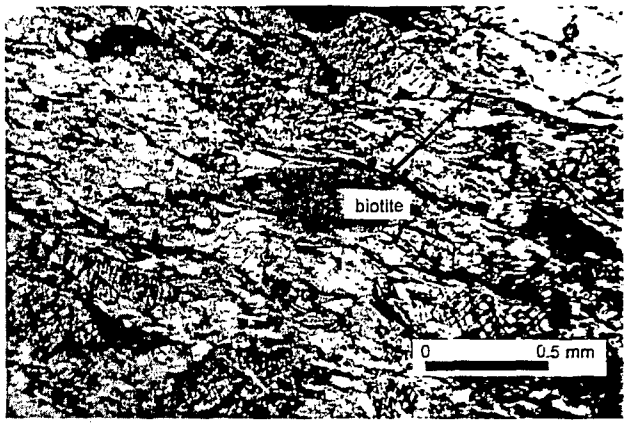

FIG. 9. Thin-section photomicrograph showing a discordant biotite porphyroblast in biotite-marble of the Mina III gold deposit (PF-CM-138-2, parallel nicols).

TABLE 1. K-Ar Analytical Data for Selected Mineral Concentrates of the Mina III Gold Deposit

Rock sample	Mineral	K, wt%	^{40}K, x 10^{-15} mol/g	^{40}Ar, x 10^{-15} mol/g	K-Ar age, Ma	$^{40}Ar/^{39}Ar$ age, Ma
Amphibole schist, K-58/351.40	amphibole	0.25	4.4942	0.2333	726 ± 16	-
Amphibole schist, K-60/380.20	amphibole, biotite	0.25 6.66	4.4942 119.7255	0.2269 4.0614	709 ± 13 506 ± 7	662.8
Amphibole schist, K-58/275.55	biotite	6.93	124.5792	4.7863	563 ± 8	575.6
Quartz-chlorite-carbonate-muscovite schist, K-20/272.35	biotite	7.26	130.5116	4.5491	518 ± 7	-
Muscovite schist, PF-CM-59-4	muscovite	7.99	143.6346	4.5685	478 ± 7	496.4
Muscovite schist, PF-CM-77-5	paragonite, chloritoid	3.36 0.22	60.4020 3.9549	2.0277 0.1555	510 ± 7 575 ± 19	497.9
Biotite-marble, PF-CM-138-2	biotite	7.59	136.4439	5.2159	561 ± 8	-

1 muscovite, and 1 paragonite) were obtained using standard procedures (jaw crushing, sieving, heavy liquids, and final hand-picking under a binocular microscope). The purity of the different separated minerals was checked both under the microscope and by X-ray diffraction. Conventional K-Ar analyses were performed on mineral separates. K was analyzed by atomic absorption and Ar measured by isotopic dilution using a ^{38}Ar spike and a modified THN 205E mass spectrometer. Between 31 and 241 mg of material was used for each experiment, as a function of K content of the sample and sensitivity of the THN 205E mass spectrometer. $^{40}Ar/^{39}Ar$ laser step-heating experiments were performed on four single grains of amphibole, biotite, muscovite, and paragonite. The laser micropobe device and procedure of the University of Nice (France) is described in Ruffet et al. (1991). The selected single grains were irradiated in the MacMaster reactor (Hamilton, Canada) for 70.30 hours with hornblende HB3GR

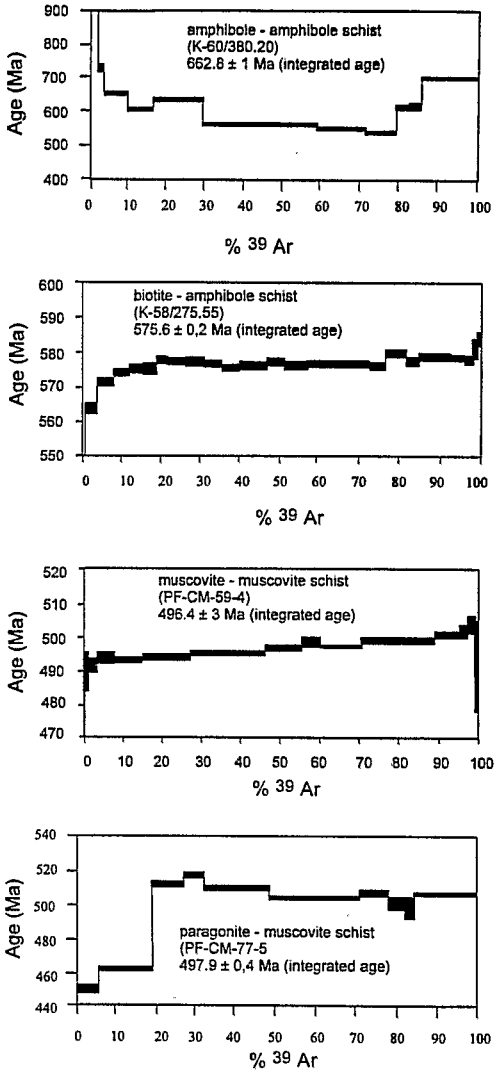

FIG. 10. $^{40}Ar/^{39}Ar$ age spectra for the Mina III gold deposit.

(1072 Ma) as a monitor. All ages were calculated using the decay constants recommended by Steiger and Jäger (1977) and are given with standard error (1σ) estimates. The errors calculated to the apparent ages of each step of temperature do not include the error of the $^{40}Ar^*/^{39}Ar$ K ratio and age of the monitor. However, the error of the $^{40}Ar^*/^{39}Ar$ K ratio of the monitor (± 0.2 to 0.5%) is included in the plateau-age error-bars calculation.

Results and Interpretations

The K-Ar isotopic data as well as the resulting ages are presented in Table 1. The amphibole and biotite porphyroblasts concentrated from the amphibole schists yielded discordant results, i.e., 726 ± 16 Ma and 709 ± 13 Ma (amphibole), and 563 ± 8 Ma and 506 ± 7 Ma (biotite). An age of 518 ± 7 Ma was obtained on the biotite porphyroblasts of the quartz-chlorite-carbonate-muscovite schist. In the muscovite schists, ages of 575 ± 19 Ma were obtained on chloritoid porphyroblasts, 510 ± 7 Ma on paragonite, and 478 ± 7 Ma on muscovite concentrates. In the biotite-marble, an age of 561 ± 8 Ma has been obtained on biotite porphyroblast concentrate.

Complete tabulated data for $^{40}Ar/^{39}Ar$ analysis are presented in Table 2, and the resulting age spectra are shown in Figure 10. The K-60/380.20 amphibole sample displays a typical saddle-shaped age spectrum characteristic of incorporation of excess argon during mineral growth. The integrated $^{40}Ar/^{39}Ar$ age is 662.8 Ma, comparable with the K-Ar age of 709 ± 13 Ma. The lowest fraction of the spectrum therefore could represent a maximum closure age of the mineral (550.9 Ma). The biotite from the same sample yielded a K-Ar age of 506 ± 7 Ma, lower than the amphibole minimum age of 550.9 Ma. $^{40}Ar/^{39}Ar$ analysis of K-60/380.20 biotite is in progress.

The K-58/275.55 biotite sample has been analyzed quite precisely through a 27-step process, although a general increase in age relative to temperature was observed. It yielded a plateau age between the steps 8 and 19 at 577.0 ± 1.2 Ma. The integrated age of 575.6 ± 0.2 Ma is in agreement with the K-Ar age of 563 ± 7 Ma.

The PF-CM-59-4 muscovite sample is characterized by a flat age spectrum gently increasing toward higher-temperature steps. No reliable plateau age can be calculated from the spectrum. However, the final high-temperature steps yield ages of 500 to 503 Ma. The integrated age is 496.4 ± 3 Ma, which is close to the K-Ar age of 478 ± 7 Ma. The heterogeneous distribution of Ar isotopes might be the result of a ^{39}Ar recoil effect induced by the very fine size of the sericite aggregates constituting the analyzed sample. This could explain why the $^{40}Ar/^{39}Ar$ ages are slightly older than the K-Ar age.

TABLE 2. $^{40}Ar/^{39}Ar$ Analytical Data by Single-Grain Laser Analysis for the Mina III Gold Deposit

Step no.	^{40}Ar atm, %	^{39}Ar K, %	^{37}Ar Ca/^{39}Ar K	$^{40}Ar^*/^{39}Ar$ K	Age, Ma	Error, ± Ma
			Amphibole schist (K-60/380.20) amphibole			
1	25.5	0.7	2.00e+01	212.04	2655.6	17.6
2	18.6	1.4	1.20e+01	115.40	1875.2	7.3
3	5.2	1.5	1.31e+01	31.30	726.2	11.7
4	2.1	6.4	1.76e+01	27.67	655.6	3.8
5	1.4	6.7	1.85e+01	25.49	611.7	3.4
6	1.0	13.1	1.91e+01	26.84	639.0	2.7
7	0.7	29.4	1.90e+01	23.47	570.0	1.6
8	0.8	12.8	1.84e+01	23.08	561.9	2.3
9	1.8	7.6	1.78e+01	22.55	550.9	3.7
10	1.4	3.7	1.78e+01	26.33	628.8	5.5
11	-	2.5	1.86e+01	26.51	632.3	7.9
Fuse	1.2	14.3	1.82e+01	30.50	711.0	3.1
Integrated age					662.8	1.0
			Amphibole schist (K-58/275.55) biotite			
1	61.8	0.1	2.87e-02	11.34	302.6	41.3
2	13.0	0.8	1.18e-02	17.41	445.9	3.4
3	3.8	3.5	2.55e-03	22.80	564.1	1.6
4	1.1	4.1	8.20e-04	23.16	571.8	1.0
5	0.7	3.7	1.10e-03	23.28	574.4	0.9
6	0.4	3.7	5.56e-04	23.34	575.6	1.1
7	0.5	3.0	6.35e-04	23.33	575.3	1.1
8	0.1	3.5	6.13e-04	23.45	577.9	1.1
9	0.3	4.2	4.05e-04	23.44	577.6	1.1
10	-	4.9	2.89e-08	23.43	577.5	1.4
11	0.2	4.6	4.97e-04	23.41	577.1	0.9
12	0.3	4.3	4.98e-04	23.36	575.9	1.0
13	0.1	3.2	5.35e-04	23.40	576.9	1.1
14	0.1	3.9	1.31e-03	23.39	576.6	1.0
15	0.2	4.4	1.60e-03	23.43	577.5	1.0
16	0.3	5.9	1.29e-03	23.39	576.6	1.0
17	0.3	7.8	2.33e-03	23.40	576.9	0.8
18	0.2	7.3	3.73e-03	23.41	577.2	1.0
19	0.1	4.0	6.54e-03	23.39	576.5	1.1
20	-	4.9	6.00e-03	23.55	580.0	0.9
21	0.2	3.3	9.02e-03	23.47	578.3	1.1
22	-	4.4	7.52e-03	23.53	579.5	1.0
23	0.2	3.3	1.02e-03	23.53	579.5	0.9
24	0.2	3.6	1.26e-03	23.50	579.0	0.8
25	-	2.0	1.71e-03	23.48	578.6	1.3
26	-	0.8	1.02e-02	23.63	581.6	2.9
Fuse	0.2	1.2	1.89e-03	23.78	584.8	1.9
Plateau age (steps 8–19)					577.0	1.2

(*continued*)

The PF-CM-77-5 paragonite age spectrum is highly disturbed in the lowest-temperature section (steps 1 to 5), while presenting a flat release pattern for steps 6 to 10. For this section, a plateau age at 504.2 ± 1.4 Ma is calculated, representing 50% of ^{39}Ar release, which is in agreement with the K-Ar age of 510 ± 7 Ma.

In conclusion, the K-Ar and $^{40}Ar/^{39}Ar$ ages obtained on the Mina III gold-mine wall-rock samples are distributed into three different groups. (1) The oldest ages (659 to 709 Ma) are obtained only on amphibole porphyroblasts and are related to excess argon (as demonstrated by $^{40}Ar/^{39}Ar$ data) incorporated in the amphibole

TABLE 2. (*continued*)

Step no.	^{40}Ar atm, %	^{39}Ar K, %	^{37}Ar Ca/^{39}Ar K	^{40}Ar*/^{39}Ar K	Age, Ma	Error, ± Ma
			Muscovite schist (PF-CM-59-4) muscovite			
1	22.8	0.1	2.00e-02	15.44	397.8	27.9
2	9.8	0.2	1.15e-02	17.92	454.2	13.1
3	1.4	1.0	2.86e-07	19.54	490.2	5.5
4	0.6	2.5	1.63e-03	19.61	491.8	1.9
5	0.1	4.4	1.97e-04	19.73	494.3	1.7
6	0.1	7.0	3.89e-08	19.70	493.6	0.9
7	0.1	12.2	7.80e-04	19.74	494.6	0.9
8	-	19.0	3.53e-04	19.78	495.4	0.7
9	-	9.4	2.91e-08	19.85	497.0	0.8
10	0.0	4.8	5.77e-08	19.92	498.5	1.4
11	-	10.5	2.61e-08	19.86	497.2	0.8
12	-	18.2	1.50e-08	19.93	498.7	1.0
13	0.2	6.0	1.79e-03	20.00	500.3	1.0
14	-	2.7	1.01e-07	20.05	501.3	1.8
15	0.2	1.3	4.10e-04	20.13	503.0	2.6
16	4.9	0.4	4.59e-02	19.20	482.7	5.5
Fuse	2.1	0.5	5.96e-02	19.81	496.1	8.3
Integrated age					496.4	0.3
			Muscovite-schist (PF-CM-77-5) paragonite			
1	1.0	5.5	3.23e-02	17.72±	451.2	2.0
2	-	13.6	4.15e-02	18.23±	462.7	0.9
3	0.1	8.2	3.87e-02	20.46±	512.1	1.6
4	0.7	5.3	3.23e-02	20.69±	517.1	1.7
5	0.2	16.2	2.10e-02	20.35±	509.7	1.0
6	0.2	22.0	1.52e-02	20.11±	504.4	0.9
7	0.1	7.7	1.48e-02	20.18±	505.9	1.8
8	0.9	3.9	1.57e-02	19.92±	500.1	3.3
9	1.3	2.1	1.48e-02	19.76±	496.7	6.0
10	0.1	15.5	1.99e-02	20.14±	505.1	1.0
Integrated age					498.0	0.5
Plateau age (steps 6–10)					504.2	1.4

crystals during their development. (2) A second group of ages, ~565 ± 15 Ma, is typical of biotites from amphibole-schists, quartz-chlorite-carbonate-muscovite schists and biotite-marble, chloritoid from muscovite schists, and amphibole porphyroblasts in the amphibole schists. (3) In a third group, ages are clustered around 500 ± 5 Ma, as defined by K-Ar and ^{40}Ar/^{39}Ar plateau ages for muscovite (slightly increasing age spectrum) and paragonite from the muscovite schist. Considering (a) that the gold mineralization at Mina III is closely associated with a mesothermal infiltration process developed at 450 ± 50° C (Fortes and Giuliani, 1995), (b) that the synchronous fluid-rock K-alteration mechanism that developed the muscovite schists is spatially associated with the massive sulfide orebodies, and (c) that there is a lack of subsequent tectonic or thermal remobilization of the mineralization, we conclude that an age of 500 ± 5 Ma may represent the best estimate of the gold-mineralizing event at Mina III.

Interpretation of the second group of ages (565 ± 15 Ma) appears to be more problematic. It characterizes porphyroblasts of amphibole, biotite, and chloritoid that have grown over pre-existing matrix minerals and which may represent the peak of the prograde regional metamorphism. The analyzed minerals have been sampled within the thermal halo of the mineralizing hydrothermal system, and therefore their developed K-Ar system might have been partially reset during this late event. A second hypothesis is that these porphyroblasts are synchronous to the gold-mineralization event (505

± 10 Ma), and that the older ages represent the effect of excess argon; the older ages, like those of the first group, probably would be geologically meaningless.

Discussion

The dating of gold deposits in greenstone belts is not an easy task because of their complex evolution in terms of magmatism, metamorphism, and deformation and also because it is not possible to determine directly the age of the minerals (generally quartz and sulfides) with which gold is preferentially associated. Whatever the genetic model adopted, gold mineralization is generally related to the late stages of the greenstone belt's metamorphism and deformation (Robert, 1990).

The metamorphic and deformational history of the Crixás greenstone belt is not simple, and its full treatment lies well beyond the scope of the present paper. However, the interpretation of the difference between the age of the analyzed porphyroblasts (amphibole, biotite, and chloritoid) and matrix minerals (muscovite and paragonite) will depend on whether it is assumed that the porphyroblasts are syn- or intertectonic, which is not always easy to distinguish (Passchier and Trouw, 1996). Field and petrographic evidence suggests that the porphyroblasts are intertectonic and that they may represent the peak of the prograde regional metamorphism, as they have grown over preexisting matrix minerals. The subsequent metamorphic hydrothermal alteration would have generated the matrix minerals (muscovite-paragonite) that lie along the main secondary foliation.

The older ages (~659 to 709 Ma) of amphibole porphyroblasts may be explained by an excess argon retained by the mineral, and therefore may be of no geological significance. For other reasons described above, the second group of ages (565 ± 15 Ma) also is difficult to interpret at this time. On the other hand, the age of 505 ± 10 Ma indicated by muscovite and paragonite that developed during the hydrothermal alteration, which generated the muscovite schist spatially related to the orebodies of the Upper Ore Zone, may be reasonably considered to represent the age of the gold mineralization.

K-Ar and $^{40}Ar/^{39}Ar$ geochronological results presented here are in general agreement with the previous Rb-Sr geochronological data (Fortes et al., 1993, 1995), which yielded isochronic ages of 731 ± 76 Ma (K-60/380.20) and 647 ± 36 Ma (K-58/275.55) for amphibole schists, 437 ± 13 Ma for quartz-chlorite-carbonate-muscovite schist (K-20/272.35), and 497 ± 48 Ma (PF-CM-138-2) for biotite-marble. These Rb-Sr results assigned, for the first time, the formation of the Mina III gold deposit in the Crixás Archean greenstone belt to the last tectono-metamorphic event registered in the region (Brasiliano orogenic event), as previously suggested by Thomson and Fyfe (1990).

Acknowledgments

The authors wish to thank Mineração Serra Grande Ltda. for access to the mine and for field support, and the Institut Français de Recherche Scientifique pour le Développement en Coopération (ORSTOM) for financial support. The authors are grateful to two anonymous reviewers for constructive comments. This is a contribution to IGCP Project No. 342, Age and Isotopes of South American Ores.

REFERENCES

Arndt, N. T., Teixeira, N. A., and White, W. M., 1989, Bizarre geochemistry of komatiites from the Crixás greenstone belt: Contrib. Mineral. Petrol., v. 101, p. 187–197.

Fortes, P. T. F. O., 1996, Metalogenia dos depósitos auríferos Mina III, Mina Nova e Mina Inglesa, greenstone belt de Crixás, Goiás: Unpubl. doctoral thesis, Inst. de Geociencias, Univ. de Brasília, 177 p.

Fortes, P. T. F. O. and Giuliani, G., 1995, Les phases fluides associées aux corps sulfurés du gisement d'or Mina II, ceinture de roches vertes de Crixás, Etat de Goiás, Brésil: Comptes Rendus, Acad. Sci. Paris, v. 320, série IIa. p. 1171–1178.

Fortes, P. T. F. O., Giuliani, G., Takaki, T., Pimentel, M. M., and Teixeira, W., 1995, Aspectos geoquímicos do depósito aurífero Mina III, greenstone belt de Crixás, Goiás: Geochim. Brasiliensis, v. 9, p. 13–31.

Fortes, P. T. F. O., Pimentel, M. M., and Teixeira, W., 1993, Geocronologia Rb/Sr das rochas encaixantes do depósito aurífero Mina III, Crixás, Goiás [abs.], *in* Volume de Resumos Expandidos do XXXVIII Congresso Brasileiro de Geologia: Brasilia, Soc. Brasil. Geol., p. 250–252.

Jost, H., and Oliveira, A. M., 1991, Stratigraphy of the greenstone belts, Crixás Region, Goiás, central Brazil: Jour. South Amer. Earth Sci., v. 4, p. 201–214.

Passchier, C. W., and Trouw, R. A. J., 1996, Microtectonics: Berlin, Springer, 289 p.

Robert, F., 1990, Dating old gold deposits: Nature, v. 346, p. 792–793.

Ruffet, G., Féraud, G., and Amouric, M., 1991, Comparison of $^{40}Ar/^{39}Ar$ conventional and laser dating of biotites from the North Trégor Batholith: Geochim. et Cosmochim. Acta, v. 55, p. 1675–1688.

Saboia, L. A., 1979, Os "greenstone belts" de Crixás e Goiás: Bol. Inform. do Núcleo Centro-Oeste, v. 9, p. 43–72.

Saboia, L. A., Teixeira, N. A., Castro, J. H. G., and Teixeira, A. S., 1981, Geologia do "greenstone belt" de Crixás (GO) e suas implicacões geotectônicas: Anais do Simpósio sobre o craton do São Francisco e suas Faixas Marginais, Parte II: Salvador, Soc. Brasil. Geol., p. 39–50.

Steiger, R. H., and Jäger, E., 1977, Subcommission on geochronology: Convention on the use of decay constants in geo- and cosmo-chronology: Earth Planet. Sci. Lett., v. 36, p. 359–362.

Thomson, M. L., 1986, Petrology of the Crixás gold deposit, Brazil: Evidence for gold associated with hydrothermal alteration subsequent to metamorphism: Proc. Gold '86, p. 284–296.

Thomson, M. L., and Fyfe, W. S., 1990, The Crixás gold deposit, Brazil: Thrust-related postpeak metamorphic gold mineralisation of possible Brasiliano-cycle age: Econ. Geol., v. 85, p. 928–942.

Yamaoka, W. N., and Araújo, E. M., 1988, Depósito de Ouro Mina III, Crixás, Goiás, *in* Schobbenhaus, C., and Coelho, C. E. S., eds., Principais Depósitos Minerais do Brasil, v. III, Capítulo XXXIV: Brasilia, Dept. Nac. Prod. Min./Comp. Vale do Rio Doce, p. 491–498.